4 PRELIMINARY HEAT EXCHANGER SIZING

4.1 Background

As has been noted, the Schmidt analysis returns poor predictions in estimating cooler and heater heat transfer, both in magnitude and form. The mass flows, on the other hand, are relatively well predicted. From experience it is reasonable to expect that the indicated efficiency of a Stirling engine is in the neighbourhood of between 40 and 50% of the Carnot value. Thus it is possible to estimate the average heat requirement, and together with the mass flows, it is then possible to determine the heat transfer coefficient, wetted area and general heat exchanger geometry. A critical factor in the performance of the engine is to limit the viscous dissipation in the heat exchangers. This will be shown later to have major impact on the deliverable power of the engine. Usually optimising the heat exchangers for highest effectiveness results in a heat exchanger of unacceptable viscous losses. It is therefore important to consider both the heat transfer and viscous dissipation concurrently.

4.2 Cooler and Heater Internal Heat Transfer

The bulk heat transfer coefficient is defined as follows:

$$\langle \dot{Q} \rangle = h_b A_w \Delta T \qquad (4.1)$$

where

$$\Delta T = T_w - \langle T_g \rangle_b$$

where $\langle T_g \rangle_b$ is the cyclic and spatial average gas bulk temperature and T_w is the average wall temperature for the heat exchanger.

The pertinent dimensionless group is the Nusselt number which is given by

$$\mathrm{Nu} = h_b d_h / k \tag{4.2}$$

which, for a given geometry and working fluid, is constant for laminar flow.

Therefore, neglecting entrance and oscillatory effects[†], the laminar flow heat transfer coefficient is a constant which depends only on the flow path geometry and working fluid.

If the flow is laminar and fully developed, the heat transfer may then be described by

$$\langle \dot{Q} \rangle = \mathrm{Nu}\, k A_w (T_w - \langle T_g \rangle_b) / d_h \tag{4.3}$$

Table 4.1 lists Nusselt numbers for various flow geometries.

Turbulent flow in situations where the flow is oscillating, as in a Stirling engine, behaves somewhat differently to what might be expected from

---

[†]Entrance effects are particularly important in a laminar flow heat exchanger. Typically, the heat exchangers tend to be fairly short, thus entrance effects must be considered at some point in the design process. Oscillatory effects are also important and will be discussed later.

Table 4.1 Laminar Flow Nusselt Numbers [Wo77]

Cross Section	d_h		Nusselt Number
		d	3.66
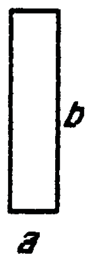	$b/a = 1$	a	2.98
	$= 1.4$	$1.17a$	3.08
	$= 2$	$1.33a$	3.39
	$= 3$	$1.5\,a$	3.96
	$= 4$	$1.6\,a$	4.44
	$= 8$	$1.78a$	5.95
	$= \infty$	$2.0\,a$	7.54
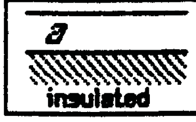		$4.0a$	4.86

purely steady state conditions. In particular, the flow is unstable in the deccelerating phase of the flow cycle and therefore once turbulence is established, it persists until the point at which the flow reverses to begin the accelerating phase. Thus if turbulence occurs, the flow will generally remain turbulent for a minimum of half the flow period. Furthermore, the point of transition is vague and unquantified. The effect of oscillatory flow on transition to turbulence is discussed in some detail in the work of Hino *et al* [HS76] and Merkli and Thomann [MT75]. In this section, in order to obtain limits of performance, it will be assumed that heat exchangers will either be all laminar or all turbulent. Of course the flow will never be entirely turbulent since it has to go through a point of zero velocity, however, if turbulence occurs early after flow reversal then it is reasonable to neglect the laminar phase.

For turbulent flow the heat transfer coefficient is slowly varying and will therefore be assumed constant. The Reynolds analogy [KK58] relates the heat transfer coefficient to the friction factor by a simple relationship which is adequate for preliminary considerations. This relationship is given by

$$\mathrm{Nu} = f\mathrm{Re}/2 \qquad (4.4)$$

where the hydraulic diameter is assumed to account for different flow geometries (in turbulent flow, geometries of similar hydraulic diameters will have similar coefficients of friction).

Thus for turbulent flow

$$\langle \dot{Q} \rangle = f \langle \mathrm{Re} \rangle k A_w (T_w - \langle T_g \rangle_b)/(2 d_h) \qquad (4.5)$$

where ⟨Re⟩ is the mean Reynolds number and is defined as follows:

$$\begin{aligned} \langle \mathrm{Re} \rangle &= \pi^{-1} \int_{hc} (\rho U d_h/\mu) d\theta \\ &= d_h (\pi \mu A)^{-1} \int_{hc} w \, d\theta \end{aligned}$$

The integration is performed over a half cycle since the heat transfer is assumed to occur to (or from) the wall in both half cycles. Thus substituting for w from either (3.67) or (3.71), the general form of the mean Reynolds number becomes

$$\langle \mathrm{Re} \rangle = d_h (\pi \mu A R \langle T_g \rangle_b)^{-1} \omega \langle p \rangle V_{sw} \qquad (4.6)$$

where V_{sw} is the respective associated swept volume, eg, for the cooler V_{sw} is V_{swc}.

Substituting (4.6) into (4.5), the turbulent heat transfer becomes

$$\langle \dot{Q} \rangle = f\omega \langle p \rangle V_{sw} k A_w (T_w / \langle T_g \rangle_b - 1)/(2\pi\mu A R) \tag{4.7}$$

Equations (4.3) and (4.7) apply directly to the cooler and heater. The respective heat transfers may be estimated from the Equations for Q_c and Q_e in Table 3.2. (65)

4.3 Regenerator Heat Transfer

For regenerator matrices there is no distinct transition point, the curves of pressure drop and heat transfer verses Reynolds number being generally monotonic [UB84]. Fortunately, in practical machines, the peak Reynolds number is generally low (Re ≈ 10) and it is usually possible to assume that pressure drop varies linearly with Reynolds number and the heat transfer varies weakly with Reynolds number. Thus Equation (4.3) may be applied to regenerators of porous matrix as well, typical data for which is given in Figure 4.1. However, before an optimum design for the regenerator can be persued, it is important to gauge its effect on the engine's overall performance. To this end, both ideal and actual regenerator heat transfers need to be estimated. Typically, the unidirectional transfer of heat in the regenerator may be as much as an order of magnitude greater than that transfered in the heater [UB84]. Thus a small ineffectiveness in the regenerator translates to a much larger effect on the engine efficiency.

Regenerator Matrices used:

	GM GPU-3	Ford 4-215
Mesh size (wires in^{-1})	200	200
Wire diameter d_m (mm)	0.04	0.036
Porosity ψ	0.697	0.618

Typical available steady flow data

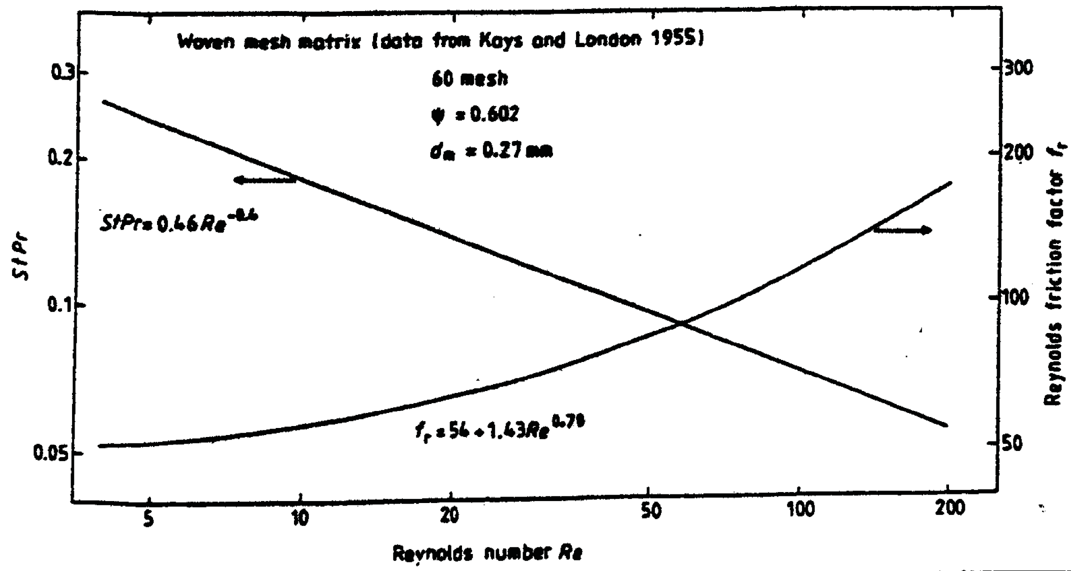

Figure 4.1 Woven Mesh Matrix: Friction Factor and Heat Transfer [UB84]. St is the Stanton number given by St = Nu/(RePr) and f_r is the Reynolds friction factor given by $f_r = f\text{Re}$.

The instantaneous heat transfer in the regenerator is given by Equation (3.22).

$$\mathrm{D}Q_r = V_r c_v \mathrm{D}p/R - c_p(T_k w_{kr} - T_h w_{rh}) \qquad (3.22)$$

Equation (3.22) may be represented in vector form to better understand how the modes of energy transfer to the regenerator interact. Figure 4.2 shows the relative relationship of regenerator heat transfer to volume and mass flow variations. It can be seen that the pressure variation term increases the required heat transfer rate over that due to pure enthalpy transport. Both the pressure variation term and the enthalpy term are of similar order, often sharing the total required heat transfer in approximately equal proportion. Note that the pressure derivative term moves the regenerator heat transfer to a closer phase with the displacer. For the example in Figure 4.2 the peak regenerator heat transfer occurs slightly leading the pressure and lagging the antiphase of the total volume. The antiphase of the volume is also a point of minimum rate of change of volume. Thus if the regenerator heat transfer is arranged to be in antiphase with the total volume then the peak regenerator heat transfer will occur when the volume is almost constant.

Equation (3.22) may be reduced to a form involving basic engine parameters. To do this, expressions for the mass flows and rate of change of pressure are required. By the same methods as outlined in S3.8 the mass flows may be evaluated to give

$$w_{kr} \approx \omega \langle p \rangle (2RT_k)^{-1}\{-[2(V_k + V_{clc}) + V_{swc}](a/S)\sin(\beta+\theta) + V_{swc}\sin\theta - V_{swc}(a/S)\sin(\beta+2\theta)\} \tag{4.8}$$

$$w_{rh} \approx \omega \langle p \rangle (2RT_h)^{-1}\{[2(V_h + V_{cle}) + V_{swe}](a/S)\sin(\beta+\theta) - V_{swe}\sin(\alpha+\theta) + V_{swe}(a/S)\sin(\alpha+\beta+2\theta)\} \tag{4.9}$$

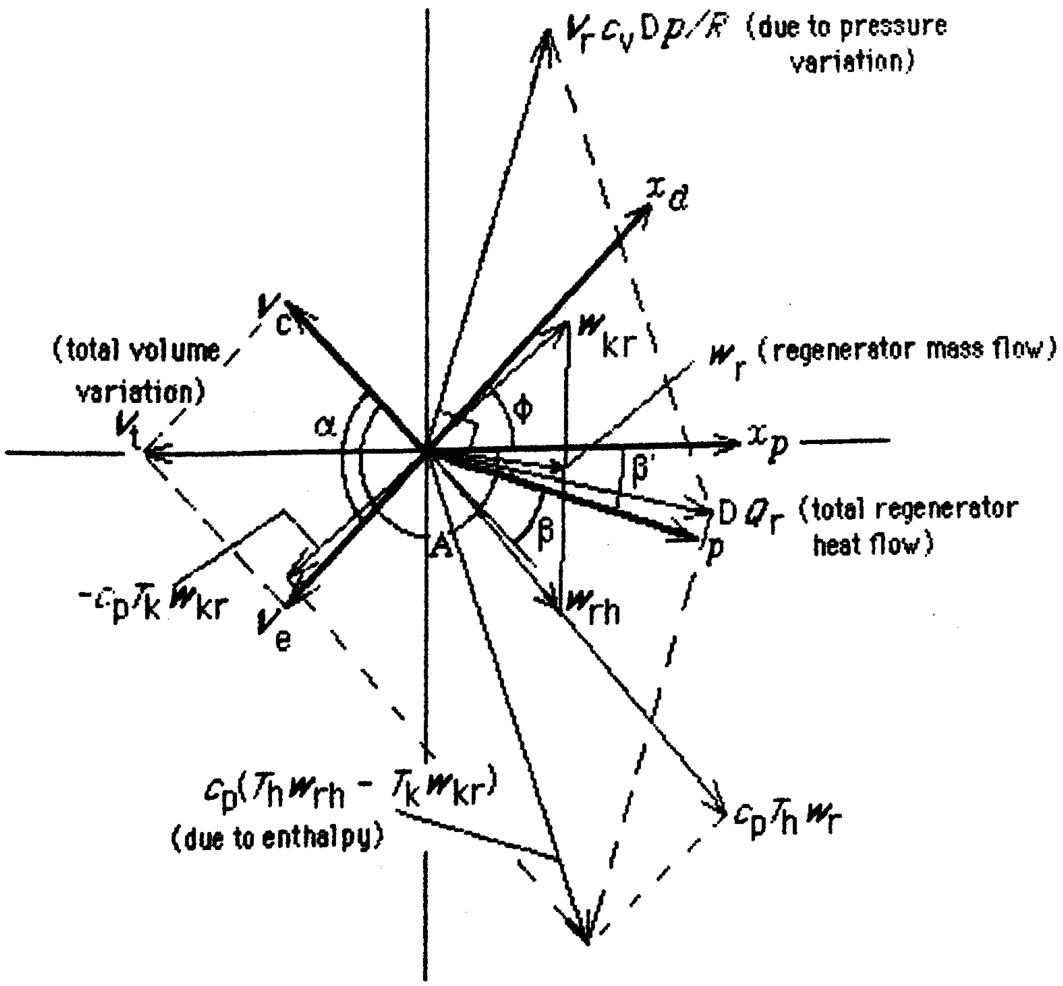

Figure 4.2 Relative Relationship of Instantaneous Regenerator Heat Transfer to Volume and Mass Flow Variations

and $\mathrm{D}p$ is given by

$$\mathrm{D}p \approx \omega \langle p \rangle (a / S)\sin(\beta + \theta) \tag{4.10}$$

where terms in $(a / S)^2$ and higher have been ignored. By substituting (4.8) through (4.10) into (3.22), an approximate solution for the ideal heat transfer rate to the regenerator is obtained.

$$D Q_r \approx \omega \langle p \rangle \gamma[2(\gamma - 1)]^{-1}\{ V_{rD}(a/S)\sin(\beta + \theta) - V_{swc}\sin\theta - V_{swe}\sin(\alpha + \theta) + (a/S)[V_{swc}\sin(\beta + 2\theta) + V_{swe}\sin(\alpha + \beta + 2\theta)]\}$$

where (4.11)

$$V_{rD} = [2 V_r/\gamma + 2(V_k + V_{clc} + V_h + V_{cle}) + V_{swc} + V_{swe}]$$

If only the first harmonic is retained, then (4.11) may be expressed in the following form:

$$D Q_r = |D Q_r|\cos(\theta + \beta_r) \qquad (4.12)$$

where

$$|D Q_r| = \omega \langle p \rangle \gamma[2(\gamma - 1)]^{-1}[V_f^2 + V_{swc}^2 + V_{swe}^2 + 2(V_{swc} V_{swe}\cos\alpha - V_f V_{swc}\cos\beta - V_f V_{swe}\cos(\alpha - \beta))]^{1/2}$$

and

$$\beta_r = \tan^{-1}[(V_{swc} + V_{swe}\cos\alpha - V_f\cos\beta)/(V_f\sin\beta - V_{swe}\sin\alpha)]$$

where

$$V_f = [2(V_r/\gamma + V_k + V_{clc} + V_h + V_{cle}) + V_{swc} + V_{swe}] a/S$$

To find the unidirectional heat flow (also referred to as the heat transferred during one blow):

$$|Q_r| = \frac{|D\,Q_r|}{\omega}\int_{\pi/2-\beta_r}^{3\pi/2-\beta_r}\cos(\theta+\beta_r)d\theta$$

$$= 2|D\,Q_r|/\omega$$

Thus

$$|Q_r| = \langle p\rangle\gamma(\gamma-1)^{-1}[\,V_t^2 + V_{swc}^2 + V_{swe}^2 + 2(\,V_{swc}\,V_{swe}\cos\alpha$$
$$- V_t\,V_{swc}\cos\beta - V_t\,V_{swe}\cos(\alpha-\beta))]^{1/2}$$

(4.13)

which is the ideal heat transferred to or from the regenerator in one blow. Equation (4.13) shows that the ideal unidirectional regenerator heat transfer is directly proportional to the mean (or charge) pressure and approximately proportional to engine internal volume. The gas specific heat ratio is also important, 40% more ideal heat transfer being required for air or hydrogen ($\gamma = 1.4$) as compared with helium ($\gamma = 1.67$).

Comparing the isothermal unidirectional regenerator heat flow with that predicted by an ideal adiabatic simulation for the GPU-3 engine reveals a difference of less than 10%. The isothermal result is 1247J compared with the ideal adiabatic simulation of 1347J [UB84]. It has been suggested by Urieli [UB84] that the definition for a Stirling engine regenerator effectiveness should be based on the unidirectional heat transfer as calculated from the ideal adiabatic simulation. If this approach is adopted, then the regenerator effectiveness or ideal heat transfer cannot be estimated *a priori* since it would have to be determined by a numerical experiment. This empirical-like approach does not seem warranted if the closed-form solution closely approximates the numerical simulation of the ideal adiabatic cycle.

The regenerator effectiveness may now be defined.

$$\epsilon = |Q_r|_{act}/|Q_r|_i \qquad (4.14)$$

where the subscripts 'act' and 'i' respectively refer to the actual and ideal unidirectional heat flows.

Most definitions of regenerator effectiveness are defined as in (4.14), however, there is a wide difference of choices and methods of evaluation for $|Q_r|_{act}$ and $|Q_r|_i$. As has been mentioned, Urieli [UB84] has suggested finding the ideal unidirectional heat flow by numerically simulating the ideal adiabatic cycle. The actual heat transfer is evaluated by Urieli from the change in enthalpy of the working gas during one blow. The use of enthalpy in this calculation may seem curious since it implies either that the change in internal energy is negligibly small or that the process occurs under approximately constant pressure conditions. Though it is true that in the ideal notion of the Stirling cycle, the processes through the regenerator are considered to occur at constant or near constant volume, in practical machines it often happens that the peak heat transfer in the regenerator occurs at or close to the minimum rate of change of pressure, thus implying a constant pressure process. From Figure 4.2 it can be seen that the regenerator heat transfer is almost in phase with the working gas pressure. The rate of change of pressure would lead the pressure by 90° (assuming sinusoidal changes), and thus be in quadrature with the regenerator heat transfer. It would appear therefore that Urieli's choice of approximating the actual regenerator heat transfer by a constant pressure process is reasonable even though it seems to violate intuition at first glance. On the other hand, the pressure is almost in antiphase with the total volume variations, and with the regenerator heat transfer leading the pressure slightly, it is possible for the peak regenerator heat transfer to occur at the point of minimum volume rate of change. Thus, in some cases, the use of a constant volume process for approximating the regenerator heat transfer is a better choice (see, for example, reference [LR84]). In the work presented here, an attempt will be made to more rigorously define the heat transfer in the regenerator in order to obtain results of wider generality.

For an engine having a non-ideal regenerator the working gas exits the hot side of the regenerator at a lower temperature than the ideal hot end temperature. Thus more heat needs to be supplied at the hot end in order to maintain the heater temperature. The hot end heat transfer is therefore given by

$$Q_e = Q_{ei} + |Q_r|_i(1 - \epsilon) \qquad (4.15)$$

where Q_{ei} is the ideal hot end heat transfer.

Similarly, when the working gas flows from the heater to the cooler, then an extra cooling load will be burdened on the cold end.

$$Q_c = Q_{ci} - |Q_r|_i(1 - \epsilon) \qquad (4.16)$$

where, again, Q_{ci} is the ideal cold end heat transfer (a negative quantity for engines).

The indicated thermal efficiency is defined by

$$\eta = (Q_e + Q_c)/Q_e$$

which, from (4.15) and (4.16) becomes

$$\eta = \eta_i/[1 + (|Q_r|_i/Q_{ei})(1 - \epsilon)] \qquad (4.17)$$

where η_i is the ideal efficiency given by (3.39), $|Q_r|_i$ is given by (4.13) and Q_{ei} is given in Table 3.2. Note here that Equation (4.17) may be used with other analyses as well. For example, Urieli has applied Equation (4.17) to predict the effects of non-ideal regenerators on the results of the ideal adiabatic analysis [UB84].

Figure 4.3 shows the effect of regenerator effectiveness as calculated by Equation (4.17) for the RE-1000 engine. In this case, if there were no regenerator, the efficiency would drop to below 10% for an isothermal engine. More importantly, it is clear that for an efficient regenerator of effectiveness approaching unity, a small reduction in effectiveness would result in a significant reduction of engine efficiency. The sensitivity of efficiency to changes in regenerator effectiveness is easily obtained by differentiating (4.17) [UB84].

$$d\eta/d\epsilon = \eta_i[1 + (|Q_r|_i/Q_{ei})(1-\epsilon)]^{-2}|Q_r|_i/Q_{ei} \quad (4.18)$$

Using this equation, it has been shown that a 1% reduction in regenerator effectiveness results in about 4% reduction in indicated efficiency for the GPU-3 engine [UB84].

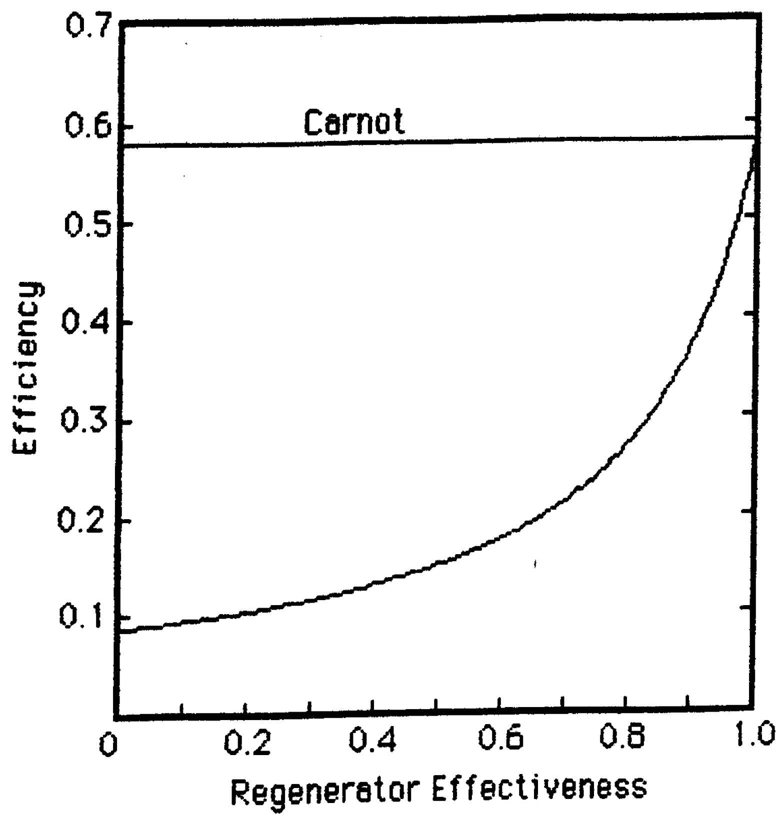

Figure 4.3 Indicated Efficiency versus Regenerator Effectiveness: Sunpower RE-1000 Free-Piston Engine.

To calculate the actual heat transfer, it is assumed that the temperature profiles of the gas and matrix are as in Figure 4.4. Regenerator temperature profiles of this approximate shape have been verified by computer simulation [Ur77, Be78] and by measurement [Be78].

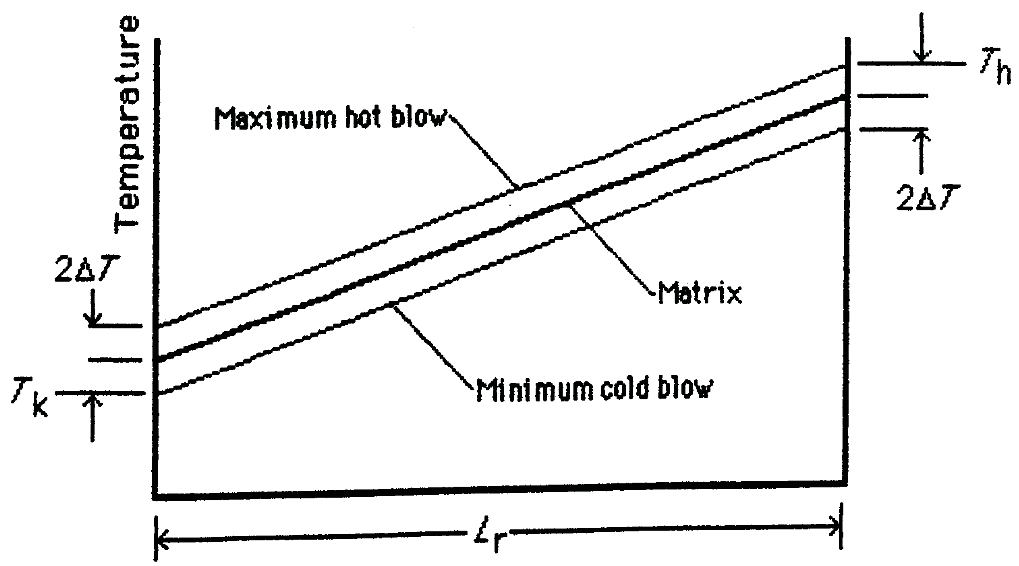

Figure 4.4 Gas and Matrix Temperature Distribution in Regenerator.

Since the gas flow is approximately in phase with the rate of heat transfer, it will be further assumed that the gas temperatures at the cold and hot ends will be in phase with the local mass flows as shown in Figure 4.5. The cold and hot end temperatures are then respectively described by

$$T_{kr} = T_k + 0.5\Delta T(1 - \sin\theta) \tag{4.19}$$

and

$$T_{rh} = T_h - 0.5\Delta T[1 - \sin(\theta + \theta_w)] \tag{4.20}$$

where for long regenerators θ_w approaches α and for short regenerators θ_w approaches 180°.

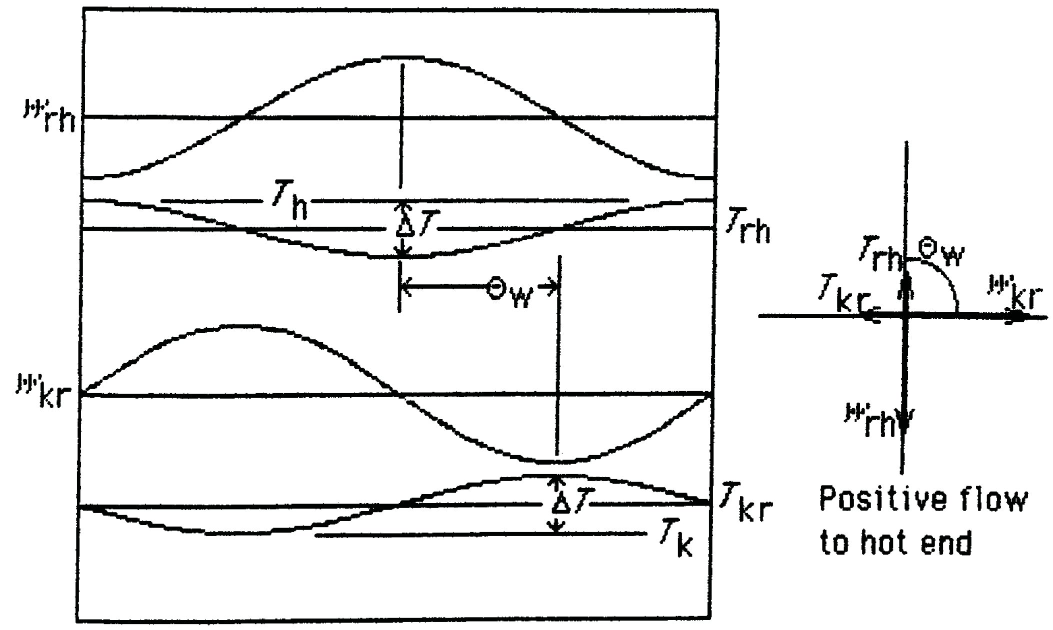

Figure 4.5 Approximate Phase Relationships between Mass Flow and Temperature

Now, assuming uniform flow over any cross-section, the spatial mean heat transfer rate is given by

$$Q_{act} \approx L_r^{-1}\int_0^{L_r} hA_w(T_w - T_g)dx \tag{4.21}$$

where T_g is the local area averaged gas temperature and, since h is slowly varying, it is treated as a constant at its mean value.

Both T_w and T_g are assumed to be linear functions of x, thus:

$$T_g = (T_{rh} - T_{kr})x/L_r + T_{kr} \tag{4.22}$$

$$T_w = (T_h - T_k - 2\Delta T)x/L_r + T_k + \Delta T \tag{4.23}$$

Substituting (4.22) and (4.23) into (4.21) and integrating, yields

$$\dot{Q}_{act} = 0.5hA_w(T_h - T_{rh} + T_k - T_{kr}) \tag{4.24}$$

which on substitution of (4.19) and (4.20) becomes

$$\dot{Q}_{act} = -0.25h\, A_w\, \Delta T\, r\sin(\theta + \theta_r) \tag{4.25}$$

where $r = \sqrt{2(1 - \cos\theta_w)}$ and

$$\theta_r = \tan^{-1}[\sin\theta_w/(\cos\theta_w - 1)]$$

Integrating (4.25) over a half cycle between zero-crossing points yields the actual heat transferred in a single blow, *viz*;

$$|Q_{act}| = h\, A_w\, \Delta T\, r/(2\omega) \quad \text{[Joules]} \tag{4.26}$$

A useful result in terms of NTU (Number of Transfer Units) may be obtained by considering the enthalpy transport through the regenerator.

Focussing on a differential length of the regenerator material in the direction of flow, as shown in Figure 4.6, an energy balance for the gas may be written as follows:

$$\Delta H + \partial Q = \mathrm{d}U.$$

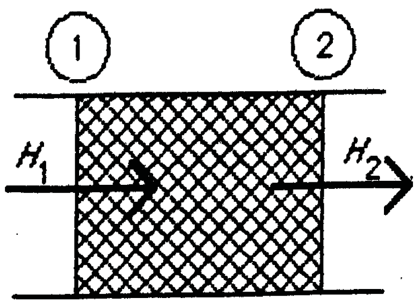

Figure 4.6 Elemental Length of Regenerator

At cyclically steady state the cyclic change in internal energy is zero, thus

$$\int \mathrm{d}U = 0$$

and from the definition of a regenerator, the heat transfer to the gas over a cycle is also zero, thus

$$\int \partial Q = 0$$

Therefore, from the energy balance, the cyclic change in enthalpy becomes

$$\int \Delta H = H_1 - H_2 = 0$$

which implies that

$$H_1 = H_2 .$$

Thus during a full period, the total amount of enthalpy transport through a cross-section in a specified direction is identical to the cyclic enthalpy transport at any other cross-section. This allows H to be evaluated at any cross-section. Therefore choosing the cold side, the cyclic enthalpy transport is given by

$$H = c_p \omega^{-1} \int_{cycle} w_{kr} T_{kr} d\theta$$

Substituting for w_{kr} and T_{kr} from (4.8) and (4.19) respectively, and noting that w_{kr} and T_{kr} are assumed to be in phase, H becomes

$$H = \pi c_p (w_{kr})_{max} \Delta T / (2\omega) \tag{4.27}$$

Now, the difference between the ideal and actual heat transfers must be equal to the enthalpy transport down the regenerator, thus

$$Q_i - Q_{act} = H \tag{4.28}$$

Dividing out by Q_{act}, (4.28) may be expressed in terms of effectiveness:

$$1/\epsilon = H/Q_{act} + 1 \tag{4.29}$$

From (4.26) and (4.27), H/Q_{act} becomes

$$H/Q_{act} = \pi c_p(w_{kr})_{max}/(h A_w r)$$
$$= \pi/(Nr)$$

where N is the NTU for the regenerator, defined as follows

$$N \equiv h A_w/[c_p(w_{kr})_{max}] \tag{4.30}$$

(4.29) may now be written in terms of effectiveness and NTU as follows:

$$\epsilon = Nr/(\pi + Nr) \tag{4.31}$$

This result allows the regenerator to be sized for thermal performance in a simple straightforward manner. Note that r varies between about $\sqrt{2}$ and 2 for θ_w between $\pi/2$ and π (r from Equation (4.25)). Since the effectiveness is improved for higher r, θ_w should be closer to π. This can be done by making the regenerator short.

Urieli and Berchowitz have used a similar result to (4.31) in ref [UB84], however, their result was based on mean mass flow rather than peak flow as used here. It is instructive to see how the two results differ.

For a sinusoidal quantity, the ratio of peak value to mean value for a half cycle is

$$s_p/\langle s\rangle = \pi/2$$

Thus the mass flows in the NTU should be in the same ratio, ie,

$$N/\langle N\rangle = \pi/2$$

Substituting this into (4.31) gives

$$\epsilon = \langle N\rangle r/(2 + \langle N\rangle r) \tag{4.32}$$

Now for short regenerators, θ_W is close to π, thus $r \approx 2$, which gives

$$\epsilon \approx \langle N\rangle/(1 + \langle N\rangle) \tag{4.33}$$

which is the result given by Urieli and Berchowitz.

Thus the Urieli and Berchowitz result is equivalent to (4.31) for regenerators that are short. For the GPU-3 machine, Equation (4.33) has been shown to give very good results [UB84]. For this machine the regenerator length was about 10% of the total length of the heat exchanger loop [UB84].

Regenerator effectivenesses in the neighbourhood of 98 to 99% are fairly typical. Using Equation (4.31), this requires an N_r value of between 154 and 311, which for short regenerators, translates to an NTU of between 77 and 156. In order to obtain such high NTU the wetted area of the regenerator is made as large as is practical. Thus porous matrices are usually the geometry of choice though some practical engines do use a simple closely spaced annular gap. The wetted area for a porous matrix is given by the following result [UB84]:

$$A_w = 4\,V_r(1 - \psi)/(d_m\psi) \tag{4.34}$$

where ψ is the porosity defined as the ratio of the void volume (V_r) to the canister (or total) volume. d_m is the wire diameter which is usually chosen as small as is practical.

The pertinent heat transfer results for all the heat exchangers are tabulated in Table 4.4.

4.4 Viscous Dissipation

In this preliminary stage it will be assumed that pressure forces are balanced entirely by viscous forces. This is not always reasonable; in some cases the inertia terms are significant and may be as much as 10 to 20% of the total pressure drop. The inertia terms are best handled by simulation which is usually done after the preliminary design has been completed.

Consider then that the pressure drop is supported by the viscous forces as follows [KK58]:

$$-dp/dx = 2f\rho U^2/d_h \tag{4.35}$$

where f is the Fanning friction factor, U is the gas velocity and d_h is the hydraulic diameter. The hydraulic diameter is defined by

$$d_h = 4A_n/z_n \tag{4.36}$$

where A_n is the free flow area per flow passage and z_n is the wetted perimeter per flow passage.

Neglecting entrance length effects, the laminar flow friction factor is given by

$$f = C_L/\mathrm{Re} \tag{4.37}$$

where Re is the Reynolds number given by

$$\mathrm{Re} = \rho U d_h/\mu.$$

From (4.35) and (4.37):

$$-dp/dx = 2\mu C_L U / d_h^2 \tag{4.38}$$

If U is replaced by the bulk spatial average velocity, then (4.38) may be approximated by

$$\Delta p = -2\mu C_L UL / d_h^2 \tag{4.39}$$

where L is the heat exchanger length.

The rate of lost work dissipated against viscous friction is given by

$$\Phi = |\Delta p A U| \tag{4.40}$$

where A is the total free flow area of the heat exchanger; $A = A_n$n, n being the number of parallel flow paths.

Substituting for Δp from (4.39), (4.40) becomes

$$\Phi = |2\mu C_L U^2 LA / d_h^2|$$

$$= |2\mu C_L U^2 V / d_h^2| \tag{4.41}$$

The time averaged dissipation is given by

$$\langle\Phi\rangle = 1/(2\pi)\int_{cycle}\Phi d\theta$$

$$= \mu C_L V/(\pi d_h^2)\int_{cycle} U^2 d\theta$$

Noting that $U = w/(\rho A)$ and using the first harmonic from the approximate mass flow (Equations (3.66)) and the pressure variation given by Equation (3.32), the laminar flow viscous dissipation for the cooler is then

$$\langle\Phi\rangle_k = \mu_k C_L V_k[\omega/(2 d_{hk} A_k)]^2[a^2 + 2ab\cos\beta + b^2] \tag{4.42}$$

where

$a = V_{swc}$ and

$b = (V_k + V_{clc} + V_{swc})(a/S)$

Since, generally for practical machines, $a/S \ll 1$ and β is around 20°, b is therefore small and may be neglected in preliminary design. In this case, the cooler laminar flow viscous dissipation becomes

$$\langle\Phi\rangle_k \approx \mu_k C_L V_k[\omega V_{swc}/(2 d_{hk} A_k)]^2 \tag{4.43}$$

Similarly, the approximate laminar flow viscous dissipation for the heater is given by

$$\langle \Phi \rangle_h \approx \mu_h C_L V_h [\omega V_{swe}/(2 d_{hh} A_h)]^2 \qquad (4.44)$$

Table 4.2 lists some laminar flow friction coefficients (C_L) for various geometries.

Table 4.2 Laminar Flow Friction Coefficients [Wo77]

Cross Section	d_h		Friction Coefficient
d (circle)		d	16.0
b, a (rectangle)	$b/a = 1$	a	14.25
	$= 1.67$	$1.25a$	15.0
	$= 2$	$1.33a$	15.5
	$= 3$	$1.5a$	17.25
	$= 4$	$1.6a$	18.25
	$= 8$	$1.78a$	19.0
	$= 10$	$1.82a$	21.25
	$= \infty$	$2.0a$	24.0
a, a (triangle)		$0.58a$	13.25

An important parameter in the design of Stirling engine heat exchangers is the heat transfer per unit flow dissipation. From Equations (4.3) and (4.43) and noting the definition for hydraulic diameter, the general form of this parameter is

$$\langle \dot{Q} \rangle / \langle \Phi \rangle = [16 k \Delta T_{wg}/(\mu \omega^2 V_{sw}^2)] n^2 \cdot (\mathrm{Nu} A_n^2 / C_L) \qquad (4.45)$$

where ΔT_{wg} is the bulk mean wall to gas temperature difference and V_{sw} is the associated swept volume.

From (4.45) it can be seen that for laminar flow the heat transfer per unit dissipation is strongly improved for a large number of parallel paths. The second group on the right hand side is defined by the choice of heat exchanger geometry. This group is tabulated in Table 4.3 for various common heat exchangers. By comparing this group for the various geometries on a per unit flow area basis, it is clear that for laminar flow, rectangular passages of high aspect ratio achieve better heat transfer per unit dissipation for equivalent internal volumes and number of parallel paths. In practical circumstances, the choice of aspect ratio is limited by the fin efficiency and engine diameter.

Table 4.3 Heat Exchanger Geometry Groups

Cross Section	A_n	$Nu\, z_n d_h / C_L$	$Nu A_n^2 / C_L$
○ d	$0.785 d^2$	$0.718 d^2$	$0.141 d^4$
$b/a = 1$	a^2	$0.836 a^2$	$0.209 a^4$
$= 2$	$2 a^2$	$1.75\ a^2$	$0.873 a^4$
$= 3$	$3 a^2$	$2.75\ a^2$	$2.07\ a^4$
$= 4$	$4 a^2$	$3.89\ a^2$	$3.89\ a^4$
$= 8$	$8 a^2$	$10.03\ a^2$	$20.07\ a^4$
$\frac{c}{a} = \infty$	ac	$0.405 ac$	$0.101 a^2 c^2$
△ a	$0.433 a^2$	$0.324 a^2$	$0.035 a^4$

The regenerator is treated a little differently. The regenerator mass flow is adequately accounted for by the mean of the cooler and heater mass flows. This is more convenient than using Equation (3.68) and appears to offer acceptable accuracy. Thus

$$w_r = (w_k + w_h)/2.$$

Using this result, the viscous dissipation for the regenerator follows similarly to that calculated for the cooler and heater, and is given by

$$\langle\Phi\rangle_r = 0.5\pi\mu C_{Lr}(\omega/d_h)^2[(V_{swc}/T_k)^2 + (V_{swe}/T_h)^2 - 2V_{swc}V_{swe}\cos\alpha/(T_k T_h)]\, T_r^2(L/A)_r \tag{4.46}$$

The assumption of a linear pressure drop (Equation (4.39)) is only accurate for short regenerators. Since there is a gas density variation in the direction of flow, it follows that for a given uniform mass flow, the gas velocity will also vary in the direction of flow. This, combined with the variation of viscosity with temperature, results in a non-linear pressure distribution. However, for most practical applications, the regenerator is short and the assumption of a linear pressure variation is reasonable. For more advanced analyses, the above effects are usually included.

For a regenerator comprised of stacked wire screens (wire diameter d_m):

$d_h = d_m\psi/(1-\psi)$ (see reference [UB84] for derivation)

Thus, for stacked wire screens the dissipation becomes

$$\langle\Phi\rangle_r = 0.5\pi\mu C_{Lr}[\omega(1-\psi)/(\psi d_m)]^2[(V_{swc}/T_k)^2 + (V_{swe}/T_h)^2 - 2V_{swc}V_{swe}\cos\alpha/(T_k T_h)]\,T_r^2(L/A)_r \tag{4.47}$$

From (4.46) and (4.47) it appears that regenerator viscous dissipation is minimum for volume phase angles (α) close to zero and maximum for volume phase angles close to 90°. Also the dissipation may be reduced for short regenerators and large free-flow areas.

Compromise between regenerator viscous dissipation and heat transfer is usually determined by the choice of d_h. Viscous dissipation is reduced for larger d_h whereas the NTU (Equation (4.30)) are improved for smaller d_h. Other considerations which would influence the optimisation of regenerator performance would include regenerator void volume and conduction losses (see S6).

For the case of turbulent flow, only the cooler and heater will be considered. Flow of high Reynolds number is unlikely in the regenerator since the resulting pressure drop would be inordinately high.

For turbulent flow, f is approximately constant. Thus from (4.35), the pressure drop becomes:

$$\Delta p = -2f\rho U^2 L/d_h \tag{4.48}$$

Thus

$$\Phi = \left| 2 f \rho U^3 L A / d_h \right| \tag{4.49}$$

which, in terms of mass flow, may be written

$$\Phi = \left| 2 f w^3 L / [(\rho A)^2 d_h] \right| \tag{4.50}$$

Since the viscous friction always opposes the flow, the lost work is always positive. Owing to the squared velocity term, Equation (4.48) is not sensitive to the direction of flow. Thus the dissipation incorrectly changes sign with changing flow direction. In order to circumvent this, some workers have introduced a product of the modulus and signed value for the squared term [Ur77, UB84]. Thus U^2 is written $|U|U$. If this method is applied to (4.50) then w^3 is written $|w|w^2$. To find the time-averaged value of the dissipation, (4.50) is integrated over the positive half of the cycle and multiplied by two. Using the approximate mass flow results, Equations (3.67) and (3.71), and the pressure from (3.32), the time-averaged turbulent flow dissipations are given by

$$\langle\Phi\rangle_k \approx \frac{f}{3\pi} \left[\frac{L}{d_h}\right]_k \frac{\langle p \rangle}{R T_k} \frac{(\omega V_{swc})^3}{A_k^2} \tag{4.51}$$

$$\langle\Phi\rangle_h \approx \frac{f}{3\pi} \left[\frac{L}{d_h}\right]_h \frac{\langle p \rangle}{R T_h} \frac{(\omega V_{swe})^3}{A_h^2} \tag{4.52}$$